Benchmark of several stochastic finite element approach for the Poisson equation

Titouan Marquaille, Arnaud Coatanhay, Thomas Bonnafont

Benchmark of several stochastic finite element approach for the Poisson equation

Titouan Marquaille, Arnaud Coatanhay, Thomas Bonnafont[(1)]
(1) Lab-STICC, CNRS UMR 6285, ENSTA, Institut Polytechnique de Paris, 29200 Brest, France

Abstract

This paper benchmarks stochastic finite element methods (SFEM) using Wiener-Askey polynomial chaos for solving the Poisson equation with uncertain permittivity in a biological cell model. We compare non-intrusive (least-squares, projection) and spectral (SSFEM) methods, using uniform random variables for the permittivity. Results show that projection and SSFEM methods accurately estimate the electric potential at a significantly reduced computational cost compared to Monte Carlo, paving the way for efficient statistical analyses. This could for example be applied to model the electroporation phenomena.

1 Introduction

Uncertainty quantification (UQ) has become increasingly important in various scientific and engineering disciplines [7] [6]. A straightforward and widely used UQ method is the Monte Carlo simulation. However, its high computational cost often limits its applicability, especially when dealing with complex models and numerous uncertain parameters.

Stochastic finite element methods (SFEM) have emerged as a powerful class of UQ techniques, particularly in the field of mechanics [2, 8]. While less prevalent in the literature, SFEM has also found applications in electromagnetism [4], offering the potential for more efficient uncertainty analysis in this domain. These methods discretize random variables via polynomial chaos expansion (PCE) [5], representing the stochastic solution with orthogonal polynomials. SFEM can be non-intrusive, treating the deterministic solver as a "black box," or intrusive, modifying the code to include the stochastic discretization.

The primary objective of this paper is to compare the performance of intrusive and non-intrusive SFEM approaches against the Monte Carlo method applied to static model of a biologic cell. Indeed, this is vital to achieve high accuracy in this case, in particular to model the electroporation phenomena [9].

Here, we first present two non-intrusive methods, the least-squares minimization method and the projection method based on Gauss quadrature, and then an intrusive one, the spectral stochastic finite element method (SSFEM). A comparative analysis, in terms of accuracy and computation times, of these methods for a realistic test case involving an electric field applied to a biological cell is also proposed. In addition, we show that using PCE it is then fast to conduct a statistical analysis, such as computing confidence interval.

2 Model and mathematical framework

Let Ω_1 be a rectangular domain, with Ω_2 and Ω_3 two subdomains such that $\Omega_3 \subset \Omega_2 \subset \Omega_1$, see Figure 1. This corresponds for example to a biological cell.

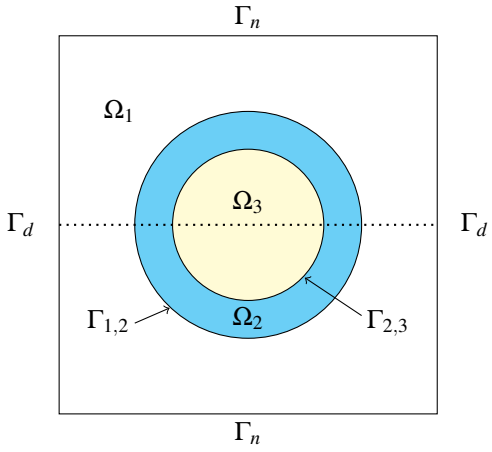

Figure 1. Geometric configuration of the model

Let $(\Theta, \mathscr{F}, \mathscr{P})$ be a probability space. In this work, we consider ε_1, ε_2, and ε_3 as random variables, denoted by $\varepsilon_1(\theta)$, $\varepsilon_2(\theta)$, and $\varepsilon_3(\theta)$ respectively, where θ represents a random event in Θ. This leads to a stochastic formulation of the problem, where the electric potential u also becomes a random variable, denoted by $u(\mathbf{x}, \theta)$, which is solution of

$$\begin{cases} -\nabla \cdot (\varepsilon_i(\theta) \nabla u_i(\mathbf{x}, \theta)) = f_i(\mathbf{x}) & \text{in } \Omega_i,\ i = 1,2,3 \\ u = 0 & \text{on } \Gamma_d \\ \frac{\partial u}{\partial \mathbf{n}} = 0 & \text{on } \Gamma_n \\ u_i = u_j & \text{on } \Gamma_{i,j} \\ \varepsilon_i \frac{\partial u_i}{\partial n} = \varepsilon_j \frac{\partial u_j}{\partial n} & \text{on } \Gamma_{i,j} \end{cases} \tag{1}$$

We work in Sobolev space $V = \{v \in H^1(\Omega) \,|\, v = 0 \text{ on } \Gamma_l \cup \Gamma_r\}$ with test functions $v \in V \otimes L^2(\Theta)$ [1], yielding a well-posed variational formulation by Lax-Milgram theorem [4].

The deterministic finite element method is unsuitable for the random variable $u(\mathbf{x},\theta)$. We thus propose to use the PCE [5], which projects the random variables onto a basis of orthogonal polynomials in the random space. Let $\xi = (\xi_1,...,\xi_N)$ be a vector of M independent random variables, here for example we have $M = 3$. The PCE of a random variable $X(\theta)$ with finite variance is obtained by

$$X(\theta) = \sum_{\alpha} x_\alpha \Psi_\alpha(\xi), \tag{2}$$

where α is a multi-index, x_α are deterministic coefficients, and $\Psi_\alpha(\xi)$ are multivariate orthogonal polynomials. The PCE is truncated to a finite degree p, resulting in a finite-dimensional space. This space contains $P = \binom{M+p}{p}$ multivariate polynomials. The choice of univariate polynomials is in general obtained from the Wiener-Askey scheme [10], relating the polynomial type to the probability distribution of the corresponding random variable (e.g., Hermite for Gaussian, Legendre for uniform).

3 Stochastic finite element methods

3.1 Non-intrusive methods

For non-intrusive methods, the main idea is to use this discretization outside the finite element without modifying existing deterministic codes (one example is Monte Carlo method). They rely on a sequential double discretization: first, a spatial discretization, analogous to the deterministic case, and then a probabilistic one.

The spatial discretization using the deterministic finite element method applied to equation (1) leads to the following approximation

$$u(\mathbf{x},\theta) \approx u_N(\mathbf{x},\theta) = \sum_{n=1}^{N} \tilde{u}_n B_n(\mathbf{x}), \tag{3}$$

where u_N approximates u in subspace V_N (basis functions $B_n(\mathbf{x})$) with nodal values $\tilde{u}_n$, and convergence is guaranteed by Cea's lemma. Assuming finite variance, we use polynomial chaos expansion on nodal values $\tilde{u}_n(\theta)$ and project onto the polynomial chaos space, analogous to spatial projection, yielding the surrogate model

$$u_{NP}(\mathbf{x},\theta) = \sum_{n=1}^{N}\sum_{p=0}^{P} \tilde{u}_n^p \Psi^p(\xi(\theta)) B_n(\mathbf{x}), \tag{4}$$

where $\xi(\theta) = (\xi_1(\theta),...,\xi_M(\theta)))$ is a vector of independent random variables with respect to the orthogonal basis. The goal is then to determine the basis coefficients $\tilde{u}_n^p$. Here we present two different methods.

3.1.1 Least-Square Minimisation method

The problem can be formulated as finding the coefficients $\tilde{\mathbf{u}}_n$ that minimize the expected squared difference between the finite element solution $u_{NP}^{(i)}$ and its PCE [3]. This expectation is approximated using an empirical mean over a set of d samples, $\mathscr{T} = \{\xi^{(i)}, i = 1,...,d\}$, leading to the discretized problem:

$$\hat{\mathbf{u}}_n = \arg\min_{\mathbf{u}_n \in \mathbb{R}^P} \frac{1}{d}\sum_{i=1}^{d}\left[\left(u_{NP}^{(i)} - \sum_{p=0}^{P}\tilde{u}_n^p \Psi^p(\xi^{(i)})\right)^2\right]. \tag{5}$$

The solution of (5) can be obtained by solving $\mathbf{A}\tilde{\mathbf{u}}_n = \gamma$, where $\gamma = \left\{u_{NP}^{(1)},...,u_{NP}^{(d)}\right\}$ is the vector of deterministic finite element solutions at each ξ^i and $\mathbf{A}$ the information matrix such that $A_{i,j} = \Psi^j(\xi^{(i)})$). The solution is given by [8]:

$$\tilde{\mathbf{u}}_n = (\mathbf{A}^T\mathbf{A})^{-1}\mathbf{A}^T\gamma. \tag{6}$$

To ensure the problem is well-posed, the number of unknown coefficients P must be smaller than the size of the experimental design, d. This problem can be seen as a compressed sensing one to optimize d [7].

3.1.2 Projection method

We present here a second method [2] to obtain the coefficients. Indeed, since the polynomial chaos is an orthonormal basis, we have

$$\tilde{u}_n^p = \frac{\mathbb{E}[\tilde{u}_n(\theta)\Psi^p(\xi(\theta))]}{\mathbb{E}[(\Psi^p)(\xi(\theta))^2]}. \tag{7}$$

The denominator can be computed analytically due to the independence of the ξ_i and the properties of orthogonal polynomials. The core challenge her lies in evaluating the numerator, $\mathbb{E}[\tilde{u}_n(\theta)\Psi^p(\xi(\theta))]$. To compute this expectation, we employ a quadrature rule tailored to the Wiener-Askey polynomial chaos corresponding to the distribution of $\xi(\theta)$. The accuracy of the Gauss quadrature depends on the degree d and the smoothness of the function being integrated. Higher degrees generally lead to higher accuracy but also increase the computational cost.

3.2 Intrusive Method: Spectral Stochastic Finite Element Method

In this section, we present an intrusive approach, where the code is completely modified to account for the uncertainty. We start with the variational form of (1)

$$\begin{aligned}\mathbb{E}\left[\int_\Omega \varepsilon(\mathbf{x},\theta)\nabla u(\mathbf{x},\theta)\cdot\nabla v(\mathbf{x},\theta)\,d\mathbf{x}\right] \\ = \mathbb{E}\left[\int_\Omega f(\mathbf{x})v(\mathbf{x},\theta)\,d\mathbf{x}\right].\end{aligned} \tag{8}$$

Then we discretize the spatial domain using Galerkin's method with basis functions $B_n(\mathbf{x})$ and represent the random variables $u(\mathbf{x},\theta)$ and $\varepsilon(\mathbf{x},\theta)$ using the PCE

$$u(\mathbf{x},\theta) \approx \sum_{n=1}^{N}\sum_{p=0}^{P} u_n^p B_n(\mathbf{x}), \Psi^p(\xi(\theta)) \tag{9}$$

and

$$\varepsilon(\mathbf{x},\theta) \approx \sum_{m=1}^{M}\sum_{\tilde{p}=0}^{\tilde{P}} \varepsilon_{m,\tilde{p}}(\mathbf{x})\Psi^{\tilde{p}}(\xi(\theta)). \tag{10}$$

Then, substituting these expansions into (8) and choosing test functions $v(\mathbf{x},\theta) = B_i(\mathbf{x})\Psi^j(\xi(\theta))$, we obtain a coupled system of equations. Using the orthogonality of the polynomial chaos basis, we obtain

$$\sum_{n=1}^{N}\sum_{p=0}^{P} u_n^p \left(\sum_{m=1}^{M}\sum_{\tilde{p}=0}^{\tilde{P}} \varepsilon_{m,\tilde{p}} \mathscr{P}^{p\tilde{p}j} \int_\Omega \nabla B_n \cdot \nabla B_i \, d\mathbf{x} \right) = \int_\Omega f B_i \, d\mathbf{x} \, \mathbb{E}[\Psi^j], \tag{11}$$

where $\mathscr{P}^{p\tilde{p}j} = \mathbb{E}\left[\Psi^p \Psi^{\tilde{p}} \Psi^j\right]$ can be pre-computed analytically. This finally leads to the following linear system

$$\mathbf{A}\,\mathrm{vec}(\mathscr{M}_u) = \mathbf{b}, \tag{12}$$

where $\mathrm{vec}(\mathscr{M}_u)$ contains the unknown coefficients u_n^p, $\mathbf{A}$ is the global stiffness matrix assembled from element contributions, and $\mathbf{b}$ is the load vector. Solving this system yields the coefficients u_n^p and thus to the desired surrogate model (9). To manage the computational cost of large matrices in high-dimensional, high P problems, strategic evaluation point selection is crucial [6].

4 Numerical Results

The goal here is to compare the presented methods using a realistic scenario . In this case, let Ω_1 be A 10x10 μm square domain, that contains a biologic cell modeled by circular subdomains Ω_2 (3.1 μm radius, cytoplasm) and Ω_3 (3 μm radius, nucleus), implicitly defining the membrane. Permittivity are modeled as uniform random variables, with $\varepsilon_1 \sim U(67,80)$, $\varepsilon_2 \sim U(2,12)$ and $\varepsilon_3 \sim U(60,80)$, from [9]. As an example we show the resulting potential distribution in the deterministic case in Figure 2.

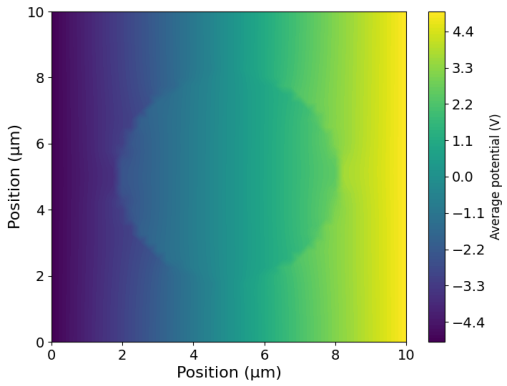

Figure 2. Potential computed on the whole domain from the deterministic method with $\varepsilon_1 = 73.5$, $\varepsilon_2 = 7$ and $\varepsilon_3 = 70$.

In Figure 3, we plot the evolution of the mean value of the potential along an equatorial cut of the cell (shown as a dotted line in Figure 1). The potential calculated using the deterministic method, evaluated here at the mean of the permittivity intervals, is also displayed. Since the two non-intrusive methods are theoretically equivalent, only the mean potential obtained from the projection method is plotted.

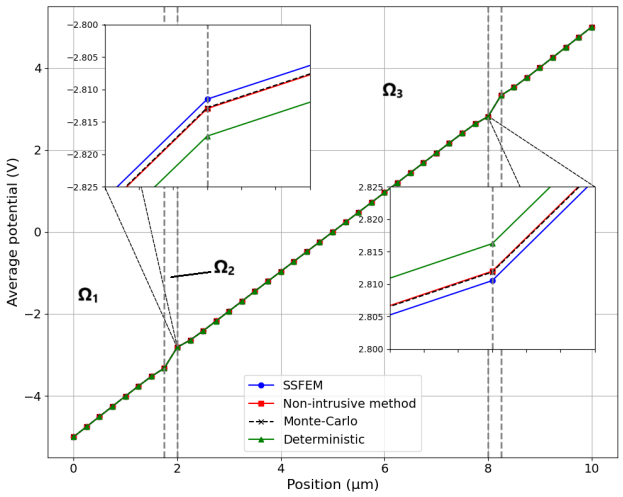

Figure 3. Comparison of the mean electric potential along the equator of the cell

As expected, Figure 3 shows that the computationally efficient SSFEM and projection methods accurately capture the mean potential, closely matching the Monte Carlo results. While the deterministic solution is accurate in Ω_1 and Ω_3, discrepancies appear in Ω_2, highlighting the impact of uncertainties. A comparison of the quadratic (Quad) and maximum (Max) errors for the potential, as well as the second-order moment (which is expected to increase the error), and the computation times for each method against Monte-Carlo is presented in Table 1.

Method	Time(s)	Quad_Pot	Max_Pot	Quad_M2	Max_M2
SSFEM	16.6	0.00008	0.00126	0.00245	0.06752
Projection	10.4	0.00002	0.00015	0.00049	0.02282
Least square	10.3	0.00002	0.00015	0.00049	0.02282

Table 1. Comparison of quadratic and maximum errors, and computation times for different methods, relative to the Monte-Carlo method.

As the table clearly shows, the high error at the membrane points visible in Figure 3 significantly affects the quadratic error. The slightly higher error of SSFEM could be due to mesh refinement or conditioning. In our case, the Monte-Carlo method took ~ 26542 seconds to converge, while the non-intrusive methods took ~ 10 seconds and the SSFEM took ~ 16 seconds, which can be further reduced by carefully choosing the points [7] [6].

As expected, the convergence time of these methods is drastically lower than Monte-Carlo. The efficiency of these methods enables statistical studies beyond the reach of

Monte Carlo, such as the 95% confidence interval shown in Figure 4, computed here using the projection method.

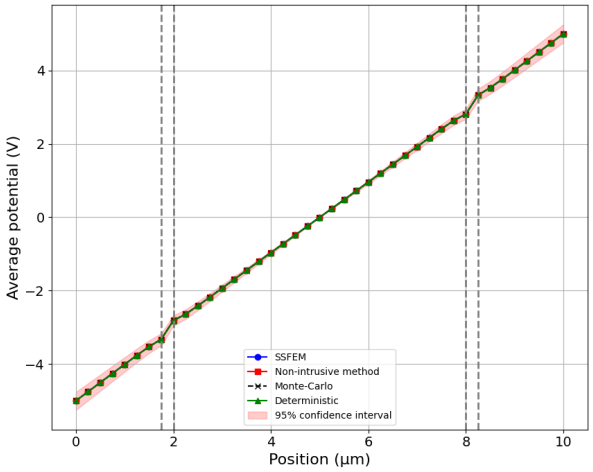

Figure 4. 95% confidence interval

Wilder confidence intervals at domain interfaces reflect permittivity discontinuities, while narrower intervals in Ω_3 suggest less potential variation. Stochastic finite element methods also provide other uncertainty metrics like failure probabilities or Sobol indices.

5 Conclusion

In this article, we compared different stochastic finite element methods to solve the Poisson equation with uncertain permittivity, modeled as uniform random variables. We applied these methods to a realistic test case of a biological cell, where the permittivity of the different domains (extracellular medium, cytoplasm, nucleus) were subject to variability. The numerical results demonstrated the efficiency of the non-intrusive methods and the SSFEM method in capturing the mean behavior of the electric potential, with an accuracy comparable to that of Monte Carlo simulations, but with a significantly reduced computational cost. They pave the way for in-depth statistical analyses, such as the determination of confidence intervals or the calculation of sensitivity indices, which would be inaccessible with Monte Carlo simulations due to their prohibitive cost.

Future work will include a better choice of interpolation points, which will reduce the error of the SSFEM when moving to a finer mesh using recently developed methods such as the Gram-Schmidt orthogonalization algorithm [6]. Our aim is to move towards higher-dimensional problems, specifically with applications in radar stealth technology. This will involve utilizing boundary finite elements, addressing the inherent complexities that arise. Moving to higher dimensions also implies working on random fields, which requires new discretization methods.

Acknowledgment

The authors would like to thank the "Région Bretagne" and ENSTA for the support of the FEARS project where this work is in progress.

References

[1] Ivo Babuska, Raul Tempone, and Georgios Zouraris. Galerkin finite element approximations of stochastic elliptic partial differential equations. *SIAM J. Numerical Analysis*, 42:800–825, 01 2004.

[2] Marc Berveiller. *Stochastic finite element analysis: intrusive and non-intrusive approaches for reliability analysis*. PhD thesis, Universite Blaise Pascal - Clermont-Ferrand II, 2005.

[3] Géraud Blatman. *Sparse and Adaptive Polynomial Chaos for Uncertainty Propagation and Sensitivity Analysis*. PhD thesis, Université Blaise Pascal - Clermont-Ferrand II, 2009.

[4] Roman Gaignaire. *Contribution to Numerical Modeling in Stochastic Static Electromagnetism*. PhD thesis, Arts et Métiers ParisTech, 2008.

[5] Roger Ghanem and John Red-Horse. *Polynomial Chaos: Modeling, Estimation, and Approximation*, pages 521–551. Springer International Publishing, Cham, 2017.

[6] Arash et al. Mohammadi. Efficient uncertainty quantification of CFD problems by combination of proper orthogonal decomposition and compressed sensing. *Applied Mathematical Modelling*, 94:187–225, 2021.

[7] Saeed Salehi, Mehrdad Raisee, Michel J. Cervantes, and Ahmad Nourbakhsh. Efficient uncertainty quantification of stochastic CFD problems using sparse polynomial chaos and compressed sensing. *Computers & Fluids*, 154:296–321, 2017.

[8] B. Sudret. Polynomial chaos expansions and stochastic finite element methods. In K.-K. Phoon and J. Ching, editors, *Risk and Reliability in Geotechnical Engineering*, chapter 6, pages 265–300. CRC Press, 2015.

[9] Thi Dan Thao Vu. *Contribution to the modeling of the electromagnetic behavior of biological media exposed to nanosecond electric field pulses*. PhD thesis, University of Limoges, 2012.

[10] Dongbin Xiu and George Em Karniadakis. The Wiener–Askey polynomial chaos for stochastic differential equations. *SIAM Journal on Scientific Computing*, 24(2):619–644, 2002.